

# Rapid Growth of Long, Vertically Aligned Carbon Nanotubes through Efficient Catalyst Optimization Using Metal Film Gradients

H. M. Christen,<sup>†,\*</sup> A. A. Puzos,<sup>‡</sup> H. Cui,<sup>†</sup> K. Belay,<sup>§</sup> P. H. Fleming,<sup>†</sup>  
D. B. Geohegan,<sup>†</sup> and D. H. Lowndes<sup>†</sup>

*Condensed Matter Sciences Division, Oak Ridge National Laboratory, Oak Ridge, Tennessee 37831, Department of Materials Science and Engineering, University of Tennessee, Knoxville, Tennessee 37996, and Department of Physics, Florida A&M University, Tallahassee, Florida 32307*

Received July 19, 2004; Revised Manuscript Received August 17, 2004

## ABSTRACT

Pulsed laser deposited, orthogonally overlapping metal film gradients are introduced as a versatile method to optimize desired nanomaterial characteristics simultaneously as a function of catalyst composition and film thickness. Catalyst libraries generated by this method are applied here to study the growth of vertically aligned carbon nanotubes by chemical vapor deposition in acetylene from Mo/Fe/Al multilayers on Si. An Fe/Mo atomic ratio of 16:1 was discovered to be optimal for the rapid growth of nanotubes to long lengths, at rates exceeding 1 mm/hr.

The characteristics of nanomaterials are known to depend strongly on the size and activity of the metal catalyst nanoparticles responsible for their growth, yet there is currently no efficient method available to systematically correlate the characteristics of the initial catalyst nanoparticles with the physical properties of the resulting nanomaterials. Systematic studies on carbon nanotubes (CNTs), in particular, are motivated by two needs: (1) to obtain aligned nanotubes with millimeter lengths to enable the formation of novel nanotube-polymer composites that incorporate continuous nanotubes throughout their thickness for highly anisotropic thermal and electrical conductivities; and (2) to provide samples for detailed physical characterization (tensile strength, thermal, and electrical conductivity, etc.).

For the growth of carbon nanostructures, the striking importance of synergistic effects in bimetallic catalysts was already recognized in early electric-arc discharge experiments<sup>1,2</sup> and confirmed in numerous more recent other studies.<sup>3,4</sup> In our own experiments on the chemical vapor deposition (CVD) growth of vertically aligned, multiwalled carbon nanotubes (MWNTs), we recently utilized time-resolved reflectivity (TRR) to explore the growth of dense MWNT arrays from e-beam evaporated multilayered cata-

lysts on Al-coated Si substrates; we often observe significant differences in growth rates and terminal lengths that are attributed to minute, unintended variations of individual catalyst thicknesses in nominally identical samples.

Metal film multilayers are an attractive choice as precursors for the catalyst nanoparticles,<sup>5-9</sup> since they permit a great number of metal catalyst combinations to be surveyed on various substrates, and several promising systems were reported.<sup>10</sup> However, systematically investigating the mechanisms responsible for the catalytic growth of carbon nanotubes is limited not only by the time-consuming nature of such study but also by run-to-run variations in subsequent processing conditions. Therefore, a method is needed that allows to efficiently perform experiments with multiple catalysts on a single sample.

In this letter, we present a new high-precision pulsed laser deposition (PLD) method designed to overcome sample-to-sample irreproducibilities, optimize rapid CNT growth to long lengths, and simultaneously determine the effects of both catalyst film composition and thickness for any two catalyst metals from which active nanoparticles for nanotube growth are formed. In this approach, two continuous, orthogonally overlapping metallic gradients (e.g., Mo and Fe) are deposited onto a substrate, so that each composition  $\text{Mo}_x\text{Fe}_{1-x}$  (for a chosen range of  $x$ ) and each total thickness  $d$  (below a chosen maximum thickness) is formed at a predetermined position on the substrate. This continuous

\* Corresponding author. E-mail christenhm@ornl.gov; phone 865-574-5965; fax 865-574-5965.

<sup>†</sup> Oak Ridge National Laboratory.

<sup>‡</sup> University of Tennessee.

<sup>§</sup> Florida A&M University.

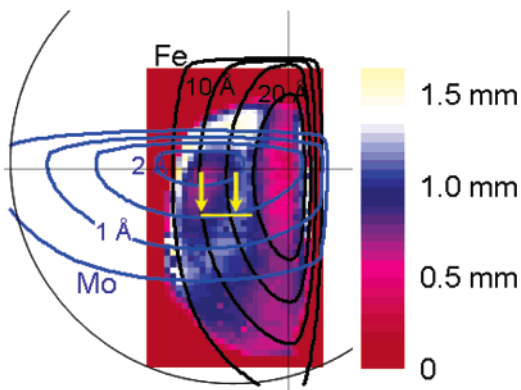


**Figure 1.** Thickness profiles of the Mo (blue solid lines) and Fe (black solid lines) catalyst layers on a 3-in. wafer, superimposed on the data of tube length as function of position on the wafer. The data were obtained by tracking the focusing height of an optical microscope. The yellow line indicates the position of the cross-section visualized in Figure 2, and the arrows indicate the location from where the TEM specimens of Figure 3 were prepared. Gas flow during the nanotube growth was from right to left.

compositional spread (CCS) method thus differs significantly from conventional combinatorial approaches,<sup>10–13</sup> where a comparatively large number of elements can be investigated, but each combination is studied with limited detail.

PLD was chosen to form the metallic gradients, as this technique permits the deposition of precisely controlled amounts of material (typically 0.01 Å per laser pulse in this work). Unlike sputtering or evaporation, PLD typically provides highly stoichiometric transfer of material from small, multicomponent targets to the substrate, can deliver material with high kinetic energies for enhanced surface chemistry, and deposition can be carried out in varying oxygen pressures to form partially or completely oxidized layers.

The substrates used in this study were prepared by e-beam evaporation of 100 Å of Al onto Si wafers, which were then transferred to the PLD system for fabrication of the catalysts. The PLD system's precise synchronization of laser firing, substrate translation, and target exchange yields controlled, wedge-shaped film thickness profiles by the deposition of the metals through a slit-shaped aperture, which is placed between the metallic target and the substrate.<sup>14</sup> The sequential deposition of Mo (bottom) and Fe (top) thus yields two overlapping profiles as shown in Figure 1, such that each point on the substrate is covered by a first layer of Mo (with a thickness  $d(\text{Mo})$ ) and a top layer of Fe (with a thickness  $d(\text{Fe})$ ). Different positions on the substrate therefore cor-

respond to different  $d(\text{Mo})/d(\text{Fe})$  ratios and different  $d(\text{Mo})+d(\text{Fe})$  amounts.

The sample was then transferred to a CVD reactor consisting of a quartz tube (3-in. diameter, 4-ft. length) placed inside a high-temperature furnace (Lindberg/Blue, model HTF55342C, 35 in. length, 8 in. uniform temperature zone). This reactor is equipped with mass flow controllers and an automatic pressure control system. The sample was heated in 25 min to 730 °C in flowing H<sub>2</sub>/Ar gas (400 sccm H<sub>2</sub>, 2000 sccm Ar) at atmospheric pressure. After this pretreatment, a preestablished 2.4 sccm flow of C<sub>2</sub>H<sub>2</sub> (Air Liquide, Alphagaz-1, 99.6% pure) was switched into the flowing Ar/H<sub>2</sub> gas mixture, thus starting the growth.

During this CVD process, a dense forest of vertically aligned nanotubes grew on the portion of the substrate containing the Fe catalyst; within this region, however, the height of the tubes depended strongly on position (thus on Mo content), as illustrated by the two-dimensional map of the forest height (Figure 1). Special attention must be paid to the potential accidental spatial variation of growth conditions (temperature, gas flow) across the wafer. Edge effects are minimized in this work by using a wafer size that is significantly larger than the area from which the data is collected, and can further be ruled out from growth experiments on wafers with uniform catalyst layers, where no significant spatial variations in tube height were observed. Analysis by scanning electron microscopy (Figure 2) shows that the tubes are continuous and well-aligned across the entire region, and that the forest height thus corresponds to the tube length.

TEM specimens were prepared with nanotubes harvested at two locations on the sample, indicated by arrows in Figure 1. As is observed in the representative images shown in Figure 3, the majority of the tubes at both locations are either single-, double-, or triple-walled (but higher numbers of walls are also present).

To better understand the dependence of tube length on catalyst composition, Figure 4 shows the data from one of the quadrants in Figure 1 as a function of  $d(\text{Mo})$  and  $d(\text{Fe})$  rather than as a function of the position. Clearly, two broad maxima are observed, one appearing near  $d(\text{Fe}) \approx 6$  Å, provided that  $d(\text{Mo}) \geq 0.3$  Å, and a second one appearing roughly along the diagonal of the plot. Obviously, this diagonal corresponds to a constant ratio  $d(\text{Mo})/d(\text{Fe})$ , and thus to a constant average alloy composition Mo<sub>x</sub>Fe<sub>1-x</sub>. It is therefore natural to represent the data of Figure 4 as a function of  $x$ .<sup>15</sup>

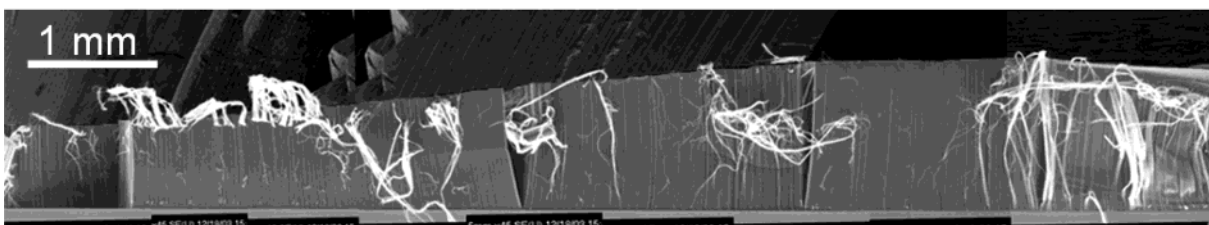


**Figure 2.** Assembly of multiple scanning electron micrographs of a cross-section across the sample in Figure 1 (images taken along the yellow line).

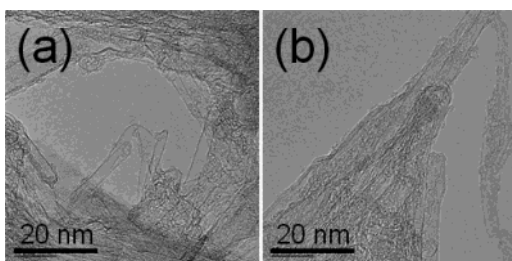


**Figure 3.** TEM images of CNTs taken at two separate positions on the sample: (a) near the local maximum (right arrow in Figure 1, average catalyst composition  $\text{Mo}_x\text{Fe}_{1-x}$  with  $x \approx 0.06$ ) and (b) near the minimum (left arrow in Figure 1,  $x \approx 0.12$ ). Most of the tubes observed on these and other images were either single-, double-, or triple-walled.

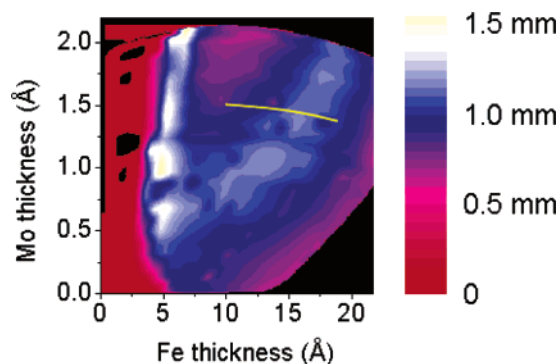


**Figure 4.** CNT length data from Figure 1 (lower left quadrant only) plotted as function of  $d(\text{Mo})$  and  $d(\text{Fe})$ . The yellow line again indicates the position of the cross-section of Figure 2.

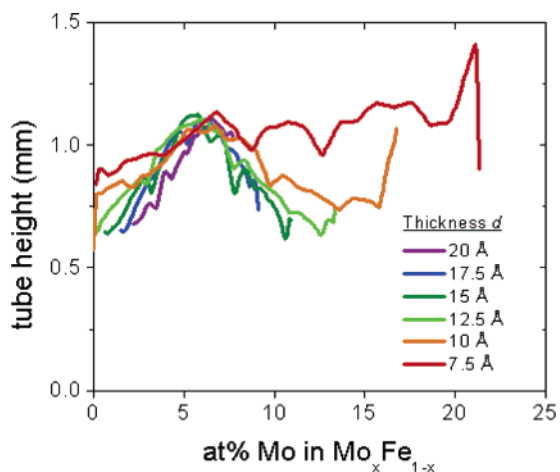


**Figure 5.** Tube length as function of  $\text{Mo}_x\text{Fe}_{1-x}$  catalyst composition  $x$ . A broad maximum is observed for  $x \approx 0.06$  independently of total catalyst thickness. For a catalyst thickness of 6–8 Å, the tube length shows only a very weak dependence on the Mo content.

Figure 5 shows a series of “cuts” through the complete data set, such as to plot the tube height as function of catalyst composition  $x$  for various values of total catalyst thickness  $d = d(\text{Fe}) + d(\text{Mo})$ . A strong local maximum in tube height is clearly observed for a composition  $x \approx 0.06$ , independent of catalyst thickness  $d$  in the range  $5 \text{ \AA} \leq d \leq 20 \text{ \AA}$ .

Closer inspection of the entire data set reveals more complex behaviors that cannot be explained simply by catalyst composition. While the data analyzed in most detail

is taken from the quadrant in which the gradients are, by design, the shallowest, interesting observations can also be made from the other portions of the sample. In fact, an apparent tendency to form long tubes is observed not only in the regions identified above but also in areas close to where the gradient of the total metal thickness is the largest. Unfortunately, it is precisely in these areas that an offset or error in the measurement of the position results in a much larger error in the determination of the catalyst composition than in the “shallow” quadrant. While these observations are the subject of further investigation, we concentrate here on the data that suffer least from such additional complications.

To verify these observations of compositional and thickness-dependent growth rates and to eliminate possible systematic errors, a second (simpler) catalyst sample was prepared under significantly different conditions. Again, a Si wafer was first coated with 100 Å of Al (as above) but then, without breaking vacuum, also was coated with a 10 Å-thick layer of Fe, with both layers deposited by e-beam evaporation. This sample was then transferred to the PLD system where a simple wedge of Mo (ranging from 0 to 2.2 Å) was deposited. Note that the order of Mo (top) and Fe (bottom) is opposite that in the previous sample with the overlapping Mo and Fe wedges. A forest of CNTs again was grown on this sample under the same conditions as above. Cross-sectional SEM imaging was used to determine the height profile, and TEM specimens were prepared by removing a bundle of tubes from different areas. Numerous nanoparticles (with typical sizes ranging from 10 to 20 nm) were located in this sample, and energy-dispersive X-ray spectroscopy (EDS) was used to determine the average composition of 10 such particles at various locations. For the tallest CNTs, this analysis yielded  $x = 0.07 \pm 0.02$ , corresponding to the ratio of metals in the bilayer film for that location, and in excellent agreement with the observation of the maximum at  $x \approx 0.06$  on the binary spread sample.

Interestingly, equilibrium phase diagrams for the Mo–Fe system (and for the Mo–Fe–C compounds) show that the solubility limit for Mo in Fe at 730 °C is  $x \leq 0.04$ , with little change as a function of carbon incorporation.<sup>16</sup> While alloy formation in nanoparticles may in principle be possible outside of the bulk equilibrium region, our data may also indicate that the nanoparticles are indeed multiphase (containing Mo- and Fe-rich regions), but have an average composition that corresponds to the metallic bilayer from which they are formed.

This significant observation of both a catalyst composition-dependent and a catalyst thickness-dependent maximization of CNT height could not easily have been obtained either by conventional single-sample experiments or by discrete combinatorial approaches. Furthermore, the continuous variation in metal layer thickness most clearly displays the abruptness with which the growth rate changes as a function of the Mo thickness (e.g., a change of  $d(\text{Mo})$  of 0.5 Å typically results in a 50% reduction in CNT height). Clearly revealing the importance of sub-Å control in the deposition of Mo, which is difficult to achieve by e-beam evaporation, thus explains the large variations in CNT growth rates that

we have previously observed on nominally identical catalyst samples. Obviously, further work is required to determine other physical properties of the resulting nanotubes, since length is only one of many factors determining the value of the obtained material.

To overcome the requirement of sub-Å deposition control for catalysts, it is promising that our results indicate that tall CNT forests can be CVD-grown rapidly by controlling only the average composition  $x$  of the  $\text{Mo}_x\text{Fe}_{1-x}$  catalyst with the thickness allowed to vary in the range of 5–20 Å (keeping in mind, however, that properties other than height have to be considered depending on the application). Formation of such a specific alloy is readily achieved by sputtering or laser-ablation from a target of that composition. This approach greatly aids ongoing research efforts in which rapid growth of vertically aligned CNT arrays to multi-millimeter lengths is desired to enable the formation of novel nanotube–polymer composites incorporating CNTs that are continuous throughout their thickness to obtain highly anisotropic thermal and electrical conductivities. Furthermore, long nanotubes also are required for detailed characterization of physical properties such as tensile strength, electrical conductivity, and thermal conductivity.

The observation of a catalyst composition and of a catalyst thickness that yield the highest growth rates also has important scientific impact. The catalytic growth of carbon nanostructures and of other nanomaterials still is poorly understood, but the clearly visualized trends in our data sets provide a reliable test bed for modeling catalytic growth processes. Further experiments using different catalyst combinations, various CVD growth conditions, and the application of this approach to the synthesis of other nanomaterials such as nanowires are expected to lead to a more detailed understanding of the basic principles governing

catalytic nanomaterial growth, as well as to significantly increased production rates.

**Acknowledgment.** Research sponsored by the U.S. Department of Energy under contract DE-AC05-00OR22725 with the Oak Ridge National Laboratory, managed by UT-Battelle, LLC.

## References

- (1) Lambert, J. M.; Ajayan, P. M.; Bernier, P.; Planeix, J. M.; Brontons, V.; Coq, B.; Castaing, J. *Chem. Phys. Lett.* **1994**, *226*, 364.
- (2) Kiang, C.-H.; Goddard, W. A., III; Beyers, R.; Salem, J. R.; Bethune, D. S. *J. Phys. Chem. Solids* **1996**, *57*.
- (3) Cassell, A. M.; Raymakers, J. A.; Kong, J.; Dai, H. *J. Phys. Chem. B* **1999**, *103*, 6484.
- (4) Liao, X. Z.; Serquis, A.; Jia, Q. X.; Peterson, D. E.; Zhu, Y. T.; Xu, H. F. *Appl. Phys. Lett.* **2003**, *82*, 2694.
- (5) Geohegan, D. B.; Puzos, A. A.; Ivanov, I. N.; Jesse, S.; Eres, G.; Howe, J. Y. *Appl. Phys. Lett.* **2003**, *83*, 1851.
- (6) Cui, H.; Eres, G.; Howe, J. Y.; Puzos, A. A.; Varela, M.; Geohegan, D. B.; Lowndes, D. H. *Chem. Phys. Lett.* **2003**, *374*, 222.
- (7) Eres, G.; Puzos, A. A.; Geohegan, D. B.; Cui, H. *Appl. Phys. Lett.* **2004**, *84*, 1759.
- (8) Delzeit, L.; Chen, B.; Cassell, A.; Stevens, R.; Nguyen, C. V.; Meyyappan, M. *Chem. Phys. Lett.* **2001**, *348*, 368.
- (9) Delzeit, L.; Nguyen, C. V.; Chen, B.; Stevens, R.; Cassell, A.; Han, J.; Meyyappan, M. *J. Phys. Chem. B* **2002**, *106*, 5629.
- (10) Ng, H. T.; Chen, B.; Koehne, J. E.; Cassell, A. M.; Li, J.; Han, J.; Meyyappan, M. *J. Phys. Chem. B* **2003**, *107*, 8484.
- (11) Chen, B.; Parker, G., II; Han, J.; Meyyappan, M.; Cassell, A. M. *Chem. Mater* **2002**, *14*, 1891.
- (12) Hwang, S.-K.; Lee, K.-D.; Lee, K.-H. *Jpn. J. Appl. Phys.* **2001**, *40*, L580.
- (13) Cassell, A. M.; Verma, S.; Delzeit, L.; Meyyappan, M. Han, J. *Langmuir* **2001**, *17*, 260.
- (14) Christen, H. M.; Ohkubo, I.; Rouleau, C. M.; Jellison, G. E., Jr.; Puzos, A. A.; Geohegan, D. B.; Lowndes, D. H. *Meas. Sci. Technol.*, submitted.
- (15) This calculation is based on the bulk densities and molar masses of Fe and Mo and the assumption that the PLD-grown layers have similar densities as the bulk.
- (16) Elliott, R. P. *Constitution of Binary Alloys, First Supplement*; McGraw-Hill: New York, 1965; p 669.

NL048856F